

## 基于归一化本征荧光信号的气溶胶分类技术研究

朱鑫琦<sup>1,2</sup>, 张佩<sup>1</sup>, 王光辉<sup>3</sup>, 陈双红<sup>4</sup>, 张建平<sup>4</sup>, 朱菁<sup>1</sup>, 黄惠杰<sup>1\*</sup><sup>1</sup>中国科学院上海光学精密机械研究所信息光学与光电技术实验室, 上海 201800;<sup>2</sup>中国科学院大学, 北京 100049;<sup>3</sup>上海镭慎光电科技有限公司, 上海 201899;<sup>4</sup>海军军医大学海军特色医学中心, 上海 200433

**摘要** 提出了一种利用归一化荧光信号对气溶胶颗粒进行分类的方法。将单个粒子的荧光信号在对应散射光信号上的归一化值分为四个区间,在四个区间内分别进行计数。将其应用于以 405 nm 激光二极管为激发光源的荧光粒子计数器,实现了对细菌、核黄素、香烟烟雾、汽车尾气、荧光微球等不同气溶胶粒子的初步分类。同时,采用主成分分析算法对实验结果进行了可视化分析。该方法可应用于微生物粒子的识别和预警,降低环境中非生物荧光粒子的干扰。

**关键词** 遥感; 气溶胶检测; 本征荧光; 归一化荧光; 气溶胶分类

中图分类号 X851 文献标志码 A

DOI: 10.3788/CJL221427

## 1 引言

气溶胶是指固体或液体颗粒物悬浮在大气中形成的相对稳定的分散体系。气溶胶可分为生物气溶胶和非生物气溶胶。生物气溶胶包括空气中的病毒、细菌及相关团聚体、真菌、花粉和动植物碎屑等<sup>[1]</sup>。生物气溶胶粒子扩散会影响农业、动物以及人体健康,甚至影响水体循环和气候<sup>[2]</sup>。

近年来,各国利用激光诱导本征荧光技术搭建了各种系统,以实现空气中颗粒物的实时监测,例如紫外-空气动力学粒径仪(UV-APS)<sup>[3]</sup>、生物战剂预警传感器(BAWS)<sup>[4]</sup>、荧光空气动力学粒径仪(FLAPS)<sup>[3]</sup>和宽带集成生物气溶胶传感器(WIBS)<sup>[5-6]</sup>等。生物粒子的本征荧光是指其固有荧光。当生物粒子中所含的荧光基团受到辐射后,会产生特定的荧光光谱。主要的荧光基团有色氨酸、核黄素、烟酰胺腺嘌呤二核苷酸(NADH)等,也有一些其他代谢物和生物分子会发出荧光<sup>[7-8]</sup>。这些装置设置有多激发波长和多个荧光通道,结合多种参数对气溶胶进行鉴别,但是成本较高且体积较大。气溶胶在不同时间和空间内的分布具有差异,因此需要研制便携式装置来对气溶胶的分布进行持续检测<sup>[9]</sup>。便携式装置一般会采用单波长的激发光源,对荧光信号进行分析,多数系统可以实现对荧光与非荧光粒子的区分,但在便携式装置上实现不同生物气溶胶类型的区分仍是一种挑战<sup>[10-11]</sup>。

在之前的研究中,我们针对生物气溶胶实时监测

应用需求,开发了一款以 405 nm 激光二极管为激发光源的荧光粒子计数器,将计数器测到的荧光粒子数目与培养法测得的细菌数目进行了对照,两者具有较好的线性一致性<sup>[12]</sup>。该仪器在实际应用时,空气中的一些荧光干扰粒子会引起仪器误报警,因此需要一种能够初步鉴别气溶胶粒子种类的方法来降低仪器的误报率。

针对这一问题,本文提出一种基于归一化荧光的方法对气溶胶粒子的类型进行初步区分。将该方法应用于荧光粒子计数器,可以降低仪器在监测生物气溶胶时的误报率。

## 2 仪器设计

### 2.1 光学设计

本文以与微生物代谢相关的核黄素和 NADH 作为目标物质,采用 405 nm 激光二极管作为光源,利用透镜组将光束准直并聚焦。仪器光路图如图 1 所示。气路方向中心线、激发光路光轴和荧光接收光路的光轴两两垂直,其交点附近区域即为光敏感区。气流将气溶胶粒子带到光敏感区,该区域为激发光束与气流的重合区,同时也是抛物面反射镜的焦点。激光照射到粒子上会被粒子散射,产生弹性散射光,当粒子为生物粒子时,同时也会激发出本征荧光。弹性散射光和荧光被抛物面反射镜收集,以平行光的形式通过二向色镜。二向色镜的反射波段为 420 nm 以下,透射波段为 420~620 nm。因此,二向色镜可以将散射光和荧

收稿日期: 2022-11-17; 修回日期: 2023-01-04; 录用日期: 2023-02-09; 网络首发日期: 2023-03-09

通信作者: \*huanghuijie@siom.ac.cn

光分离。随后,散射光和荧光分别被两个光电倍增管 (PMT)接收。在荧光接收光路中设置一片有色玻璃

(牌号为JB450)作为滤光片,用于滤除散射光。在光电倍增管的光敏面之前分别设置光阑用于消除杂散光。

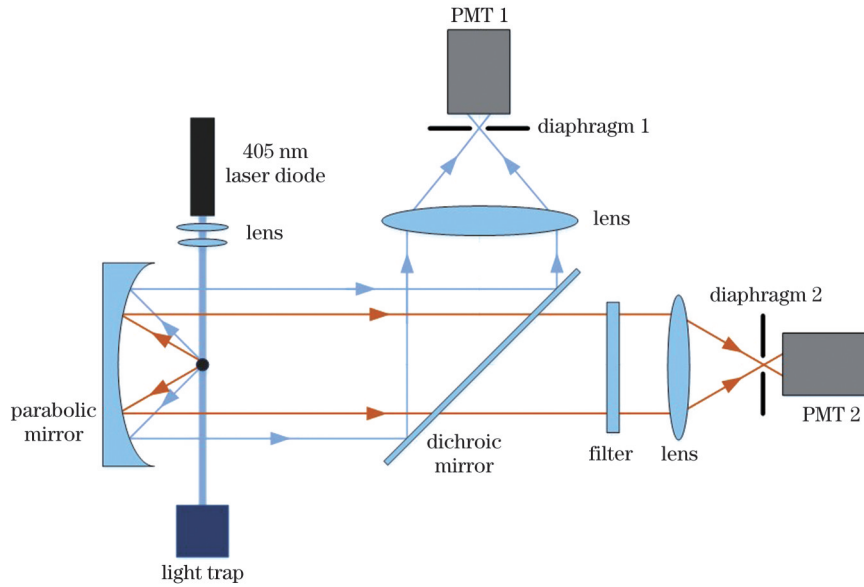


图 1 仪器光路示意图

Fig. 1 Optical path schematic of instrument

### 2.2 信号处理电路

光电倍增管会将探测到的散射光和荧光信号转化为电流信号,通过 I/V 转换后得到电压信号,再经逐级放大后被模数转换器(ADC)转化为数字信号传输至现场可编程门阵列(FPGA)中进行计算。信号处理和分析过程如图 2 所示。气溶胶粒子通过光检测区,依据米氏理论可以从这个信号中估计出粒子

(球形当量)的大小<sup>[7]</sup>。利用标准聚苯乙烯微球对仪器进行标定,对粒径为 0.5 μm 以上的粒子进行计数,总粒子数记为  $N_s$ 。而对于另一路荧光信号的检测,只有荧光粒子才会产生荧光脉冲。因此,为了降低荧光检测的噪声,只有当同时测到散射光和荧光脉冲时,才将该脉冲计入荧光脉冲总数,即荧光粒子数  $N_f$ ,否则将其忽略。

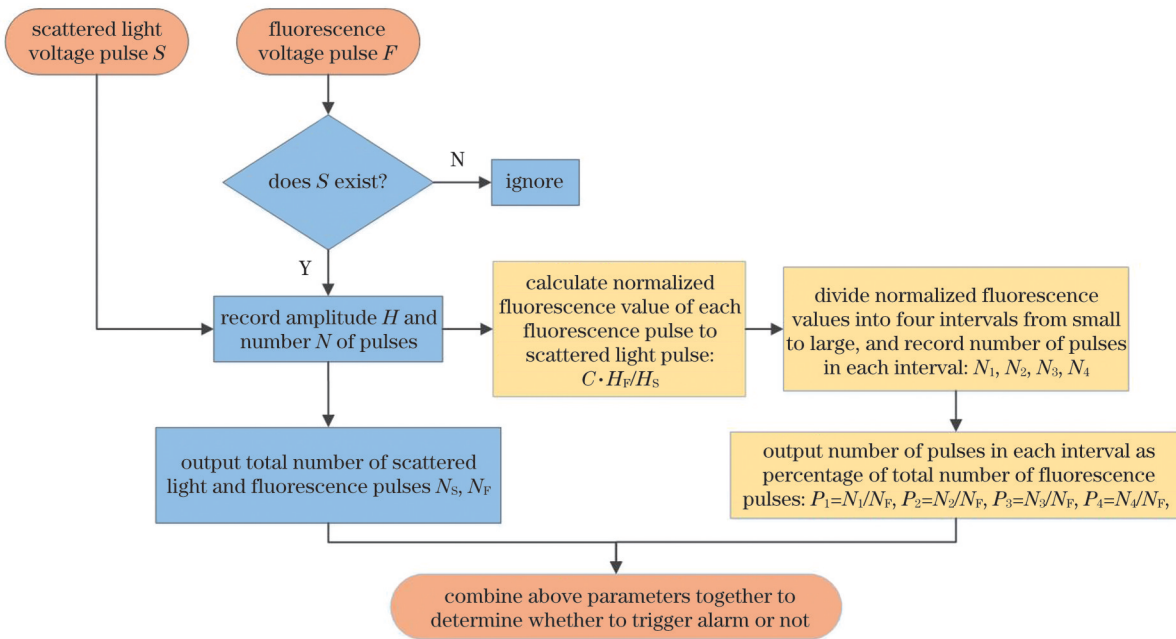


图 2 信号处理与数据分析流程图

Fig. 2 Flow chart of signal processing and data analysis

### 2.3 归一化荧光值计算

对于每个荧光脉冲幅值  $H_f$  及其对应的散射光脉

冲幅值  $H_s$ , 可以定义其归一化荧光值  $H_{NF}$  为

$$H_{NF} = C \cdot H_f / H_s, \quad (1)$$

式中:  $C$  为设定的常数。

散射光强度实际上是粒径的函数, 而将荧光强度与散射光强度相比, 可以在一定程度上减小粒径对荧光强度的影响。由于散射光幅值一般比荧光幅值大, 因此为了计算方便, 可以选用一个常数  $C$  使归一化荧光值简化为一个大于 1 的数。

计算归一化荧光值的主要目的是更好地地区分微生物气溶胶和其他气溶胶。基于此, 我们对各种气溶胶粒子进行了大量的实验测试, 确定了四个归一化荧光值区间, 由小到大分别是:  $<40$ 、 $40\sim 80$ 、 $80\sim 600$ 、 $>600$ 。值得注意的是, 区间范围的值与设置的常数  $C$  有关, 在此设置  $C=256$ 。

计算每组脉冲对应的归一化荧光值, 记录落入每个区间内的荧光粒子数  $N_1$ 、 $N_2$ 、 $N_3$ 、 $N_4$ 。

总荧光粒子数与每个区间内的荧光粒子数有如下关系:

$$N_F = N_1 + N_2 + N_3 + N_4. \quad (2)$$

计算每个区间内荧光粒子数占总荧光粒子数的比例:

$$P_i = \frac{N_i}{N_F} (i = 1, 2, 3, 4). \quad (3)$$

由此得到了每个周期内的总粒子数  $N_S$ 、总荧光粒

子数  $N_F$  以及粒子的归一化荧光值分别落在四个区间内的荧光粒子数。仪器可以结合以上参数综合判断是否触发警报。

### 3 实验结果与分析

#### 3.1 荧光与非荧光粒子

采用粒径为  $0.5 \mu\text{m}$  的单分散的聚苯乙烯乳胶 (PSL) 微球、磷酸盐缓冲液 (PBS)、粒径为  $0.8 \mu\text{m}$  的荧光微球 (B800, Thermo Scientific) 作为检测对象, 对仪器对于荧光与非荧光粒子的分类能力进行评价。其中 PBS 在生物化学研究中常用于调节 pH 值、保护生物活性, 是细菌活化和培养过程中的重要溶剂。测试时, 使用一台气溶胶发生器使样品溶液产生不同浓度的气溶胶, 将产生的气溶胶导入一个足够体积的缓冲瓶中形成稳定的体系。使用荧光粒子计数器对瓶中的气溶胶样品进行检测。表 1 为实验结果。我们记录了仪器对不同浓度样品测得的单位体积的总粒子数和总荧光粒子数, 单位为  $\text{L}^{-1}$ ; 计算了总荧光粒子数与总粒子数的比值。可以看出, PSL 微球和 PBS 中几乎不存在荧光粒子, 荧光粒子数占总粒子数的比例趋近于 0, 而 B800 作为一种荧光微球, 其荧光粒子数占总粒子数的 84% 以上。因此, 仪器可以有效区分荧光与非荧光粒子。

表 1 对荧光与非荧光粒子的鉴别结果

Table 1 Identification results of fluorescent and non-fluorescent particles

Sample	Total number of particles $N_S/\text{L}^{-1}$	Total number of fluorescent particles $N_F/\text{L}^{-1}$	$N_F/N_S/\%$
PSL microspheres	4536	0	0
	20255	0	0
	27396	0	0
PBS	4208	0	0
	17961	4	0.02
	24795	4	0.01
B800	5570	4681	84.03
	18818	16686	88.67
	25907	23379	90.24

#### 3.2 生物气溶胶与其他气溶胶分类

虽然仪器能够准确区分荧光粒子与非荧光粒子, 但能被激发出荧光的粒子既包括生物气溶胶, 也包括一些含芳香烃等有机化合物的非生物气溶胶粒子<sup>[13]</sup>。在生物气溶胶监测应用中, 这类非生物气溶胶经常会对检测结果造成干扰, 导致仪器误报警。

我们对枯草芽孢杆菌、大肠杆菌两种细菌进行了检测。菌液使用前, 需将其中的培养基等成分分离出来 (即洗脱), 将经过两次离心洗脱后的菌液稀释于 PBS 中。枯草芽孢杆菌是一种革兰氏阳性菌, 大肠杆菌是一种革兰氏阴性菌, 二者细胞壁的组成成分和结构不同。将核黄素和 B800 荧光微球分别溶于纯水中制成均匀的溶液或悬浊液。核黄素与细菌代谢相关, B800 荧光微球可以受激发射出较强的荧光, 代表空气

中可能存在的部分荧光干扰粒子。将以上溶液置于气溶胶发生器上分别产生目标气溶胶。香烟烟雾和汽车尾气是生活环境中常见的干扰物。香烟烟雾气溶胶样品是在一定空间内将香烟点燃后形成的, 将仪器置于该空间内直接进行检测。汽车尾气检测样品为汽车燃油不完全燃烧时产生的尾气, 将仪器放置于距排气口  $0.5 \text{ m}$  距离内进行检测。被测空气样品为普通办公环境空气。

利用仪器对上述每种样品进行检测, 记录 12 组不同浓度样品的检测结果, 结果如图 3 所示。FPGA 中的数据处理算法如 2.3 节中所述, 计算每组荧光-散射脉冲的归一化荧光值, 并将其分为四个区间, 计算每个区间内的荧光粒子数及其占总荧光粒子数的比例。将结果表示为柱状图, 纵坐标为每个区间的荧光粒子数占总

荧光粒子的百分比。图 3 表明:枯草芽孢杆菌和大肠杆菌的荧光粒子大多分布在区间 2、3,各区间的比例略有不同;核黄素样品 96% 以上的荧光粒子分布在区间 3 中;空气中 80% 以上的荧光粒子分布在区间 3,13% 的

荧光粒子分布在区间 2;香烟烟雾样品 98% 以上的荧光粒子分布在区间 3;汽车尾气中 84% 以上的荧光粒子分布在区间 1;B800 表面有一定的荧光染料,属于强荧光粒子,其 89% 以上的荧光粒子分布在区间 4。

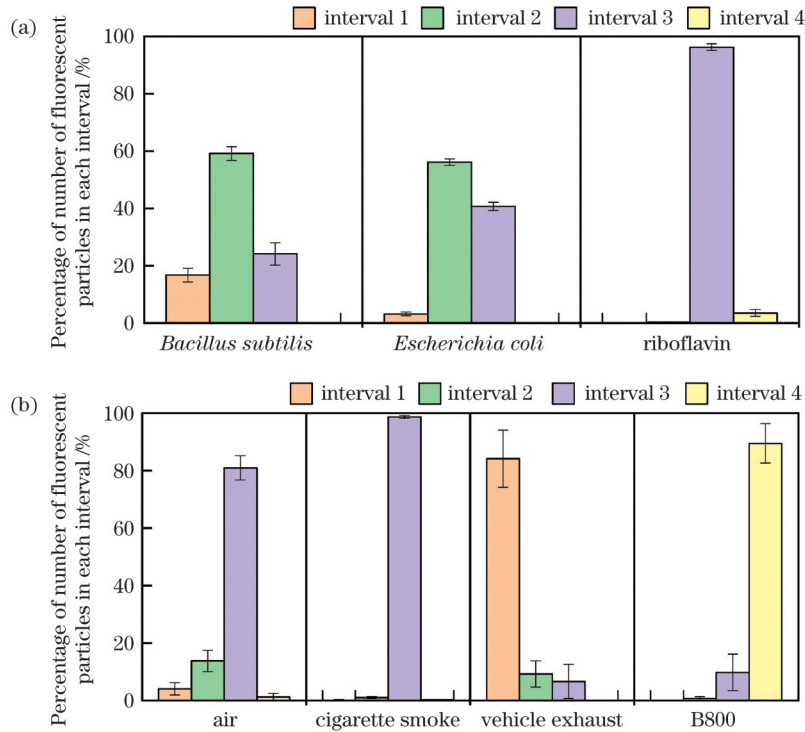


图 3 仪器对多种样品的检测与分类结果。(a) 枯草芽孢杆菌、大肠杆菌、核黄素;(b) 空气、香烟烟雾、汽车尾气、B800

Fig. 3 Detection and classification results for different samples. (a) *Bacillus subtilis*, *Escherichia coli*, riboflavin; (b) air, cigarette smoke, vehicle exhaust, B800

由以上结果可以看出,不同种类的气溶胶样品的荧光粒子数在四个区间内具有不同的分布,因此可以通过检测和计算每种样品的归一化荧光值来实现对气溶胶的分类。

### 3.3 分类可视化

主成分分析(PCA)作为一种数据降维算法,常用于光谱数据的特征提取<sup>[14]</sup>。其实现方式是计算数据矩阵的协方差矩阵,得到该矩阵的特征值和特征向量,选择特征值最大的  $k$  个特征向量,将数据矩阵转换到  $k$  个特征向量构建的新空间中,从而得到降维后的数据。PCA 可以使样本在低维空间的投影尽可能分开,是一种多维数据的图形表示方法<sup>[15-16]</sup>。

利用 PCA 对图 3 中得到的不同样品在四个区间内的荧光粒子数进行可视化分析。通过计算可以得到三个主成分(PC)PC1、PC2 和 PC3,三者的贡献率分别为 40.85%、34.47% 和 24.67%。图 4 为不同气溶胶样品在前两个主成分(PC1 和 PC2)上的得分图,二者的贡献率相加为 75.32%,已经包含了大部分的信息,在图上显示出较好的聚类效果。图 5 为三维得分图,可以将分类结果展示得更加明显。其中值得注意的是细菌与环境干扰物的分类结果。枯草芽孢杆菌、大肠杆菌和香烟烟雾以及汽车尾气的得分分布区域

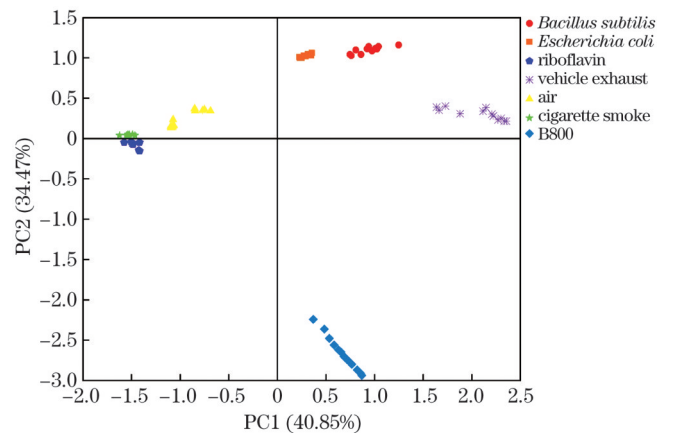


图 4 主成分分析二维得分图

Fig. 4 Two-dimensional score plot of principal component analysis

有明显的区别。核黄素和香烟烟雾的聚集区域相近,但前者一般不会直接存在于空气中,因此不会对实际环境检测结果造成干扰。B800 能够与其他样品较好地地区分开来。空气样品是一个复杂的多种粒子混合样品,因此在图中的聚集区域独立于其他样品。总之,借助 PCA 更加直观地展现出了各种气溶胶粒子的分类情况。

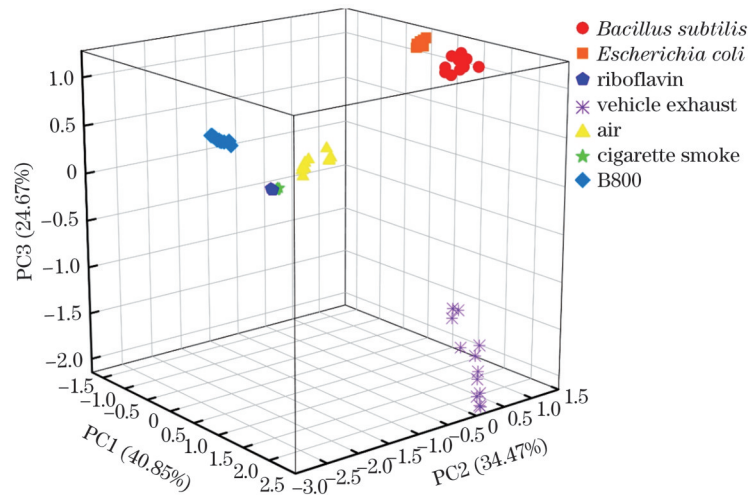


图 5 主成分分析三维得分图

Fig. 5 Three-dimensional score plot of principal component analysis

## 4 结 论

本文提出了一种基于归一化荧光信号对气溶胶粒子进行初步分类的方法。搭建了一种便携式荧光粒子计数器,以 405 nm 激光二极管为激发光源,利用 PMT 对荧光和散射光分别接收,结构紧凑,成本较低。

采用了 PSL 微球、PBS 和 B800 荧光微球对仪器对于荧光与非荧光粒子的区分能力进行了验证,通过对比其总荧光粒子数与总粒子数的比值,可以分辨荧光与非荧光粒子。对枯草芽孢杆菌、大肠杆菌、核黄素、空气、香烟烟雾、汽车尾气和 B800 荧光微球 7 种气溶胶样品进行了检测,对其单个粒子的荧光信号在对应散射光信号上进行归一化处理,将归一化荧光值分为四个区间,对单位时间内每个区间的荧光粒子数进行累计,得到每种样品的荧光粒子数区间分布。进一步采用 PCA 对数据进行了降维和可视化分析。结果显示,所提方法可以有效区分不同类型的气溶胶颗粒。

## 参 考 文 献

- [1] Forde E, Gallagher M, Foot V, et al. Characterisation and source identification of biofluorescent aerosol emissions over winter and summer periods in the United Kingdom[J]. Atmospheric Chemistry and Physics, 2019, 19(3): 1665-1684.
- [2] 朱首正, 卜令兵, 刘继桥, 等. 机载高光谱分辨率激光雷达探测大气气溶胶光学特性及污染研究[J]. 中国激光, 2021, 48(17): 1710003.  
Zhu S Z, Bu L B, Liu J Q, et al. Study on airborne high spectral resolution lidar detecting optical properties and pollution of atmospheric aerosol[J]. Chinese Journal of Lasers, 2021, 48(17): 1710003.
- [3] Hairston P P, Ho J, Quant F R. Design of an instrument for real-time detection of bioaerosols using simultaneous measurement of particle aerodynamic size and intrinsic fluorescence[J]. Journal of Aerosol Science, 1997, 28(3): 471-482.
- [4] Lynch E J, Bogucki M I, Gardner P J, et al. Biological agent warning sensor (BAWS): laser-induced fluorescence as the joint biological point detection system trigger[J]. Proceedings of SPIE, 2005, 5795: 75-78.
- [5] Foot V E, Kaye P H, Stanley W R, et al. Low-cost real-time multiparameter bio-aerosol sensors[J]. Proceedings of SPIE, 2008, 7116: 71160I.
- [6] Kaye P H, Hirst E, Foot V, et al. A low-cost multichannel aerosol fluorescence sensor for networked deployment[J]. Proceedings of SPIE, 2004, 5617: 388-398.
- [7] Kaye P H, Stanley W R, Hirst E, et al. Single particle multichannel bio-aerosol fluorescence sensor[J]. Optics Express, 2005, 13(10): 3583-3593.
- [8] Pöhlker C, Huffman J A, Pöschl U. Autofluorescence of atmospheric bioaerosols: fluorescent biomolecules and potential interferences[J]. Atmospheric Measurement Techniques, 2012, 5(1): 37-71.
- [9] 毛前军, 金穗穗. 2009 年至 2018 年全球气溶胶光学厚度时空分布特性研究[J]. 激光与光电子学进展, 2021, 58(3): 0301001.  
Mao Q J, Jin S S. Investigation of spatial and temporal distribution characteristics of global aerosol optical depth from 2009 to 2018[J]. Laser & Optoelectronics Progress, 2021, 58(3): 0301001.
- [10] 张志强, 宋凤民, 张秦, 等. 气溶胶微生物粒子计数器光学系统设计[J]. 中国激光, 2021, 48(7): 0707002.  
Zhang Z Q, Song F M, Zhang Q, et al. Design of optical system of aerosol microbial particle counter[J]. Chinese Journal of Lasers, 2021, 48(7): 0707002.
- [11] Choi K, Ha Y, Lee H K, et al. Development of a biological aerosol detector using laser-induced fluorescence and a particle collection system[J]. Instrumentation Science & Technology, 2014, 42(2): 200-214.
- [12] Lu C Y, Zhang P, Wang G H, et al. Accurate measurement of airborne biological particle concentration based on laser-induced fluorescence technique[J]. Journal of Aerosol Science, 2018, 117: 24-33.
- [13] Sivaprakasam V, Huston A L, Scotto C, et al. Multiple UV wavelength excitation and fluorescence of bioaerosols[J]. Optics Express, 2004, 12(19): 4457-4466.
- [14] 孔德明, 陈红杰, 陈晓玉, 等. 三维荧光光谱结合稀疏主成分分析和支持向量机的油类识别方法研究[J]. 光谱学与光谱分析, 2021, 41(11): 3474-3479.  
Kong D M, Chen H J, Chen X Y, et al. Research on oil identification method based on three-dimensional fluorescence spectroscopy combined with sparse principal component analysis and support vector machine[J]. Spectroscopy and Spectral Analysis, 2021, 41(11): 3474-3479.
- [15] Kaliszewski M, Włodarski M, Młyńczak J, et al. A new real-time bio-aerosol fluorescence detector based on semiconductor CW excitation UV laser[J]. Journal of Aerosol Science, 2016, 100: 14-25.
- [16] Pan Y L, Hill S C, Pinnick R G, et al. Dual-excitation-wavelength fluorescence spectra and elastic scattering for differentiation of single airborne pollen and fungal particles[J]. Atmospheric Environment, 2011, 45(8): 1555-1563.

# Study of Aerosol Classification Technique Based on Normalized Intrinsic Fluorescence Signal

Zhu Xinqi<sup>1,2</sup>, Zhang Pei<sup>1</sup>, Wang Guanghui<sup>3</sup>, Chen Shuanghong<sup>4</sup>, Zhang Jianping<sup>4</sup>, Zhu Jing<sup>1</sup>,  
Huang Huijie<sup>1\*</sup>

<sup>1</sup>Laboratory of Information Optics and Optoelectronic Technology, Shanghai Institute of Optics and Fine Mechanics, Chinese Academy of Sciences, Shanghai 201800, China;

<sup>2</sup>University of Chinese Academy of Sciences, Beijing 100049, China;

<sup>3</sup>Shanghai Lasensor Optoelectronics Technology Co., Ltd., Shanghai 201899, China;

<sup>4</sup>Center of Naval Special Medicine, Naval Medical University, Shanghai 200433, China

## Abstract

**Objective** Biological aerosols include viruses, bacteria and related agglomerates, as well as fungi, pollen, plant and animal debris. The diffusion of bioaerosol particles will seriously affect the development of agriculture and the health of animals and human beings, and even water circulation and climate. In recent years, using laser-induced intrinsic fluorescence, researchers have constructed various optical instruments to enable real-time monitoring of particulate matter in the air. The carefully designed devices use multiple excitation wavelengths and fluorescence channels, so they enable aerosol identification with multiple parameters, but exhibit drawbacks of high cost and bulky appearance. As for portable devices, there is usually a single-wavelength excitation light source to excite the fluorescence signal, and the discrimination between fluorescent and non-fluorescent particles is achieved in most devices. However, it is still a challenge to achieve discrimination between different bioaerosol types with portable devices. In our previous work, we developed a fluorescent particle counter and there was a great linear consistency between the number of fluorescent particles measured by the counter and the number of bacteria measured by the culture method. In the practical application of this counter, some fluorescent interfering particles in air possibly trigger false alarms. In this work, we propose a method for preliminary differentiation of aerosol particle types based on normalized fluorescence, and apply it to the fluorescent particle counter, which will effectively reduce the false alarm rate of the instrument while monitoring biological aerosols.

**Methods** We designed a fluorescent particle counter with a 405 nm laser diode as the light source and lens group to collimate and focus the excitation light beam. The optical axis of the excitation light path is perpendicular to the optical axis of the fluorescence receiving light path, and there is a photosensitive zone near their intersection. The airflow brings the aerosol particles to the photosensitive zone. The laser light will be scattered by the particles to produce elastic scattered light, and there will also be intrinsic fluorescence excited with biological particles. The scattered light is separated from the fluorescence using a dichroic mirror and received by two photomultiplier tubes (PMTs). The ratio of the fluorescence pulse amplitude of each particle signal to its corresponding scattered light pulse amplitude is calculated to obtain the normalized fluorescence value (Fig. 2).

**Results and Discussions** Polystyrene latex (PSL) microspheres, phosphate buffer solution (PBS), and fluorescent microspheres were used as detection objects to evaluate the instrument's ability to classify fluorescent and non-fluorescent particles. From the experimental results, we found that there are almost no fluorescent particles in PSL microspheres and PBS, and the proportion of fluorescent particles in the total number of particles tends to be close to 0, while the fluorescent microspheres exhibit fluorescent particles with >84% of the total number of particles (Table 1). Therefore, the instrument can effectively distinguish between fluorescent and non-fluorescent particles. Seven samples including *Bacillus subtilis*, *Escherichia coli*, riboflavin, B800 fluorescent microspheres, cigarette smoke, vehicle exhaust, and general office ambient air, were tested using the instrument, and the results of 12 groups of samples with different concentrations were recorded. The normalized fluorescence values of each group of fluorescence-scattering pulses were calculated and divided into four intervals, and the number of fluorescent particles in each interval and their proportions to the total fluorescent particles were calculated. The results show that the fluorescence particle numbers of different kinds of aerosol samples have different distributions in the four intervals, so the classification of aerosols can be achieved by detecting and calculating the normalized fluorescence values of each sample (Fig. 3). The obtained fluorescence particle numbers of the different samples within the four intervals were visualized using principal component analysis (PCA). With a summed contribution of 75.32%, the first two principal components (PC1 and PC2) of different aerosol samples already contain most of the information and show a good clustering effect on the graph (Fig. 4). The classification results could be more visually presented with three-dimensional score plot (Fig. 5).

**Conclusions** In this paper, we proposed a method to classify aerosol particles using normalized fluorescence signals, which was applied to a fluorescent particle counter with a 405 nm laser diode as the excitation light source, allowing preliminary classification of different aerosol particles such as bacteria, riboflavin, cigarette smoke, vehicle exhaust, and fluorescent microspheres. The normalized values of the fluorescence signals of individual particles on the corresponding scattered light signals were divided into four intervals and counted in each of the four intervals. The experimental results were visualized using PCA. This method can be applied to the identification and early warning of microbial particles, and reduce the interference of non-biological fluorescent particles in the environment.

**Key words** remote sensing; aerosol detection; intrinsic fluorescence; normalized fluorescence; aerosol classification